NASA TM X-1466

DESIGN AND OPERATION OF A HIGH-TEMPERATURE TUNGSTEN-MESH GAS HEATER

By Byron L. Siegel

Lewis Research Center
Cleveland, Ohio

NATIONAL AERONAUTICS AND SPACE ADMINISTRATION

For sale by the Clearinghouse for Federal Scientific and Technical Information
Springfield, Virginia 22151 – CFSTI price $3.00

DESIGN AND OPERATION OF A HIGH-TEMPERATURE TUNGSTEN-MESH GAS HEATER

by Byron L. Siegel

Lewis Research Center

SUMMARY

A high-temperature electrically heated gas heater was designed and is operational. This heater uses interwound helical tungsten coils as mesh heating elements. The heater has heated 0.450 and 0.69 pound per second (0.204 and 0.314 kg/sec) of nitrogen to 4530° and 4200° R (2520° and 2330° K) with average mesh bank surface temperatures as high as 4430° and 4270° R (2460° and 2370° K), respectively.

The design of the heater is described and its advantages are discussed. Problem areas associated with the design of a high-temperature heater, such as flow bypass, are described, and resulting solutions or recommendations are given.

INTRODUCTION

The Lewis Research Center, as part of the experimental phase of a tungsten water-moderated nuclear rocket concept, conducted research to evaluate reactor fuel elements. The use of preheated hot gas was chosen as the method to achieve test temperatures approaching 5000° R (2780° K). The availability of existing electric power supplies made it desirable to heat the gas electrically if heating elements with the proper electric resistance could be obtained. These elements also had to be capable of transferring large quantities of heat to the gas and withstanding the pressure drop associated with the flow rates of interest. A commercially available mesh consisting of interwound helical coils of tungsten wire was investigated for use as the heating elements. This mesh has been successfully used as the heating elements for high-temperature vacuum furnaces. The heat-transfer and pressure-drop characteristics of this type mesh is reported in reference 1. On the basis of the heat-transfer correlation obtained from this reference, the mesh heating elements were chosen. The design and operation of a gas heater using these elements is described in this report.

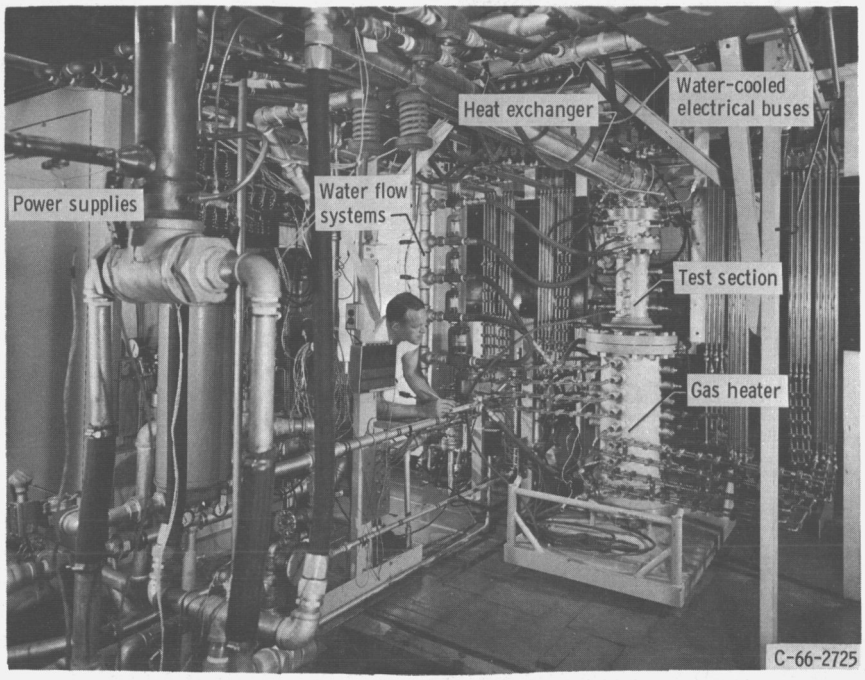

Figure 1. - Gas heater facility.

DESCRIPTION OF GAS-HEATER FACILITY

Figure 1 shows the following major components of the gas-heater facility: gas heater, test section, heat exchanger, water-cooled electric busing, power supplies, and two water flow systems. The heater consists of four banks of electrically heated mesh elements through which the gas passes in series. The flow systems, power supplies, and instrumentation associated with this heater are shown schematically in figure 2. A more detailed description of the components of these systems is given under the corresponding subheadings.

Heater

The gas heater is composed of four banks of electrically heated mesh heating elements. Each bank is electrically heated by an individually controlled power supply, the description of which is given in the section, Power Supplies. A typical heater bank shown in figure 3 is composed of two water-cooled copper buses, two molybdenum buses, two boron nitride housings, and six to eight mesh heating elements with associated molybdenum wedges and bolts.

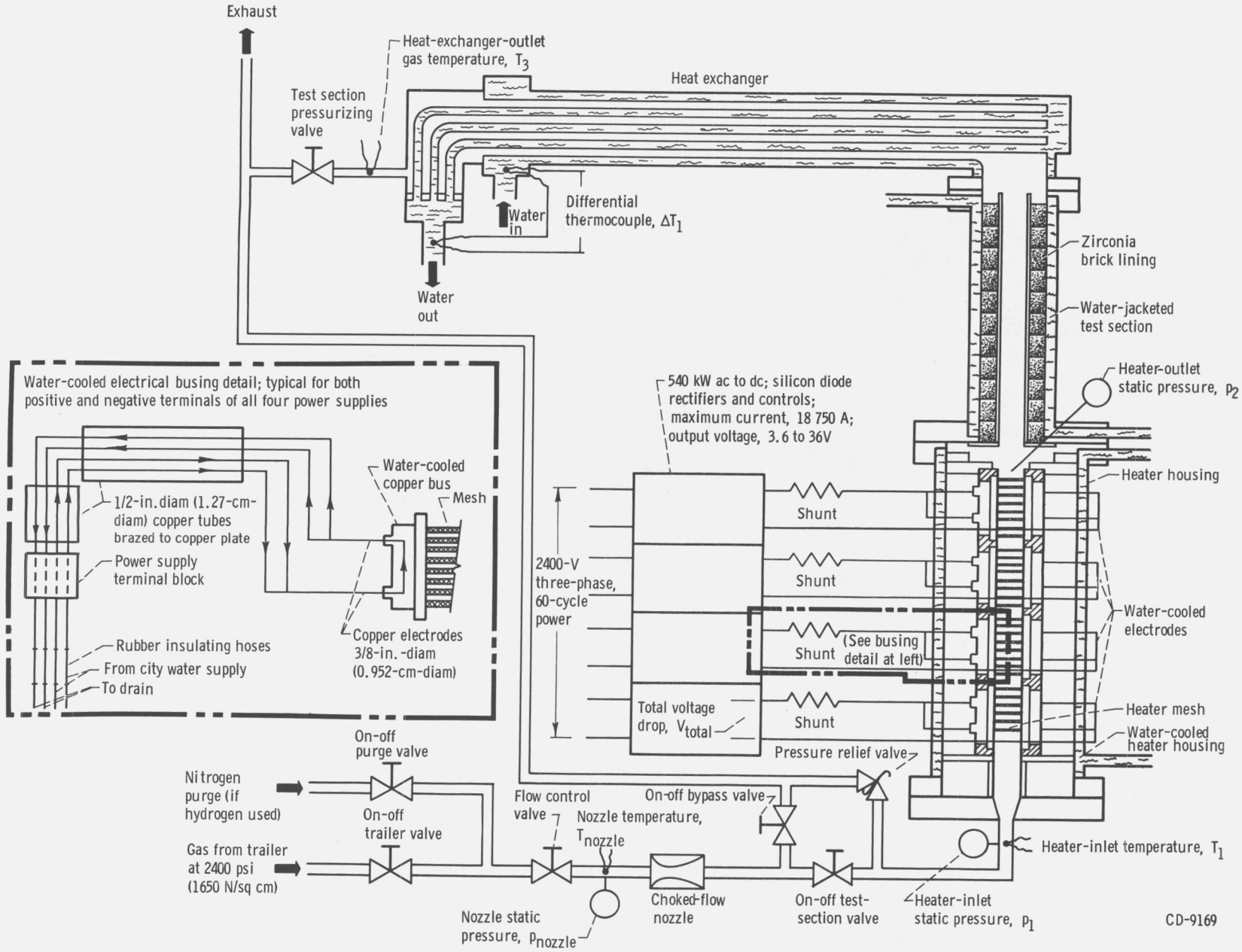

Figure 2. - Flow system, test section, and instrumentation.

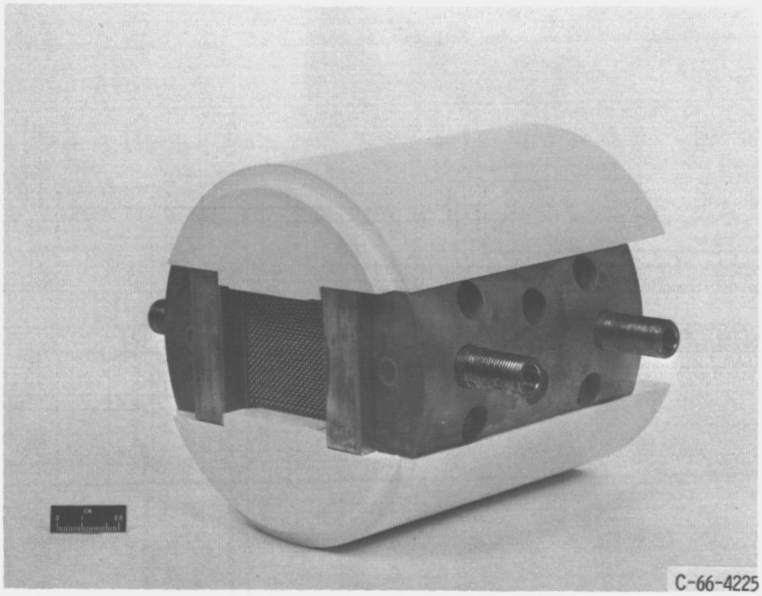

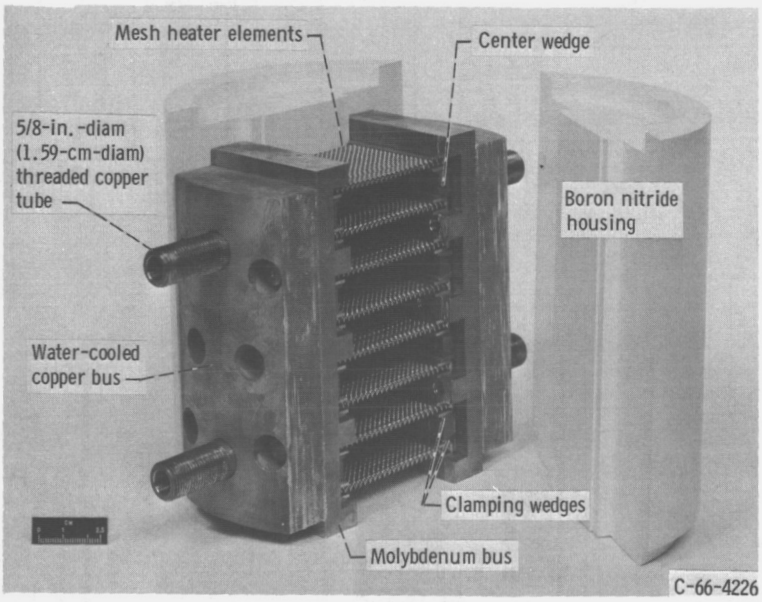

Figure 3. - Heater bank and components.

The mesh is formed by interwound helical coils of tungsten wire as shown in figure 4. The coils are sandwiched between two tungsten plates approximately 0.060 inch (0.152 cm) thick. The ends of the coils are heliarc welded to the plates to provide positive electrical connections. The mesh elements are clamped between the molybdenum buses by the wedge arrangement shown in figure 3. The larger center wedge is tightened against the two smaller clamping wedges by two bolts located behind the molybdenum buses. Counterbored holes are so located in the copper buses that the heads of the bolts which are not shown do not extend beyond the surface.

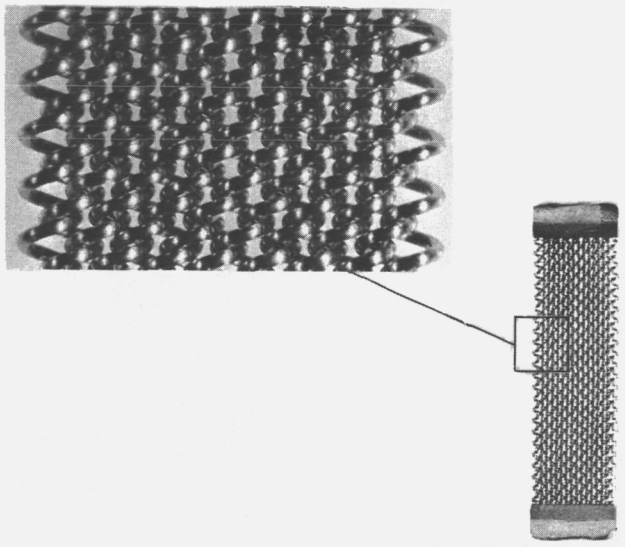

C-65943

Figure 4. - Interwound tungsten-wire-mesh heating element.

Water-cooled copper buses, with 3/8-inch-diameter (0.952-cm-diam) flow passages, are then bolted to the back side of the molybdenum buses with molybdenum bolts, the heads of which are recessed in counterbored holes within the copper buses and can be seen in figure 3. The gas flow passage is formed by the walls of the buses on two sides and boron nitride electrical insulating pieces on the other two sides. The outside surfaces of both the boron nitride housings and the water-cooled copper buses have a 3-inch (7.62-cm) radius (fig. 3). Except for 1/64-inch (0.0397-cm) clearance between the mesh and the boron nitride side walls on each side, the mesh heating elements completely fill the 2- by $2\frac{1}{8}$-inch (5.08- by 5.40-cm) rectangular flow channel formed by the busing and the boron nitride.

Figure 5 shows an isometric view of the entire heater assembly. The heater is housed in a 12-inch-inside-diameter (30.5-cm-i.d.) stainless-steel water-jacketed housing 34 inches (86.4 cm) long. As can be seen in the lower cutaway view of figure 5, the banks of meshes comprising the heater assembly are stacked on top of each other. A boron nitride electric insulating spacer is placed between the copper and molybdenum buses of each bank of meshes to form a complete cylinder, which is approximately 28 inches (71 cm) long (fig. 6). This figure was an early photograph which does not have the circular copper busing used in the final design. The boron nitride housings forming two of the sidewalls of the heater assembly are interlocking. Initially, these sidewalls were free to expand axially relative to the two sides of the heater formed by the water-cooled busing. During heater operation the differences in axial expansion between the sidewalls created gaps in the cylindrical heater assembly. These gaps allowed the gas to bypass rather than flow through the heater. The most significant portion of the

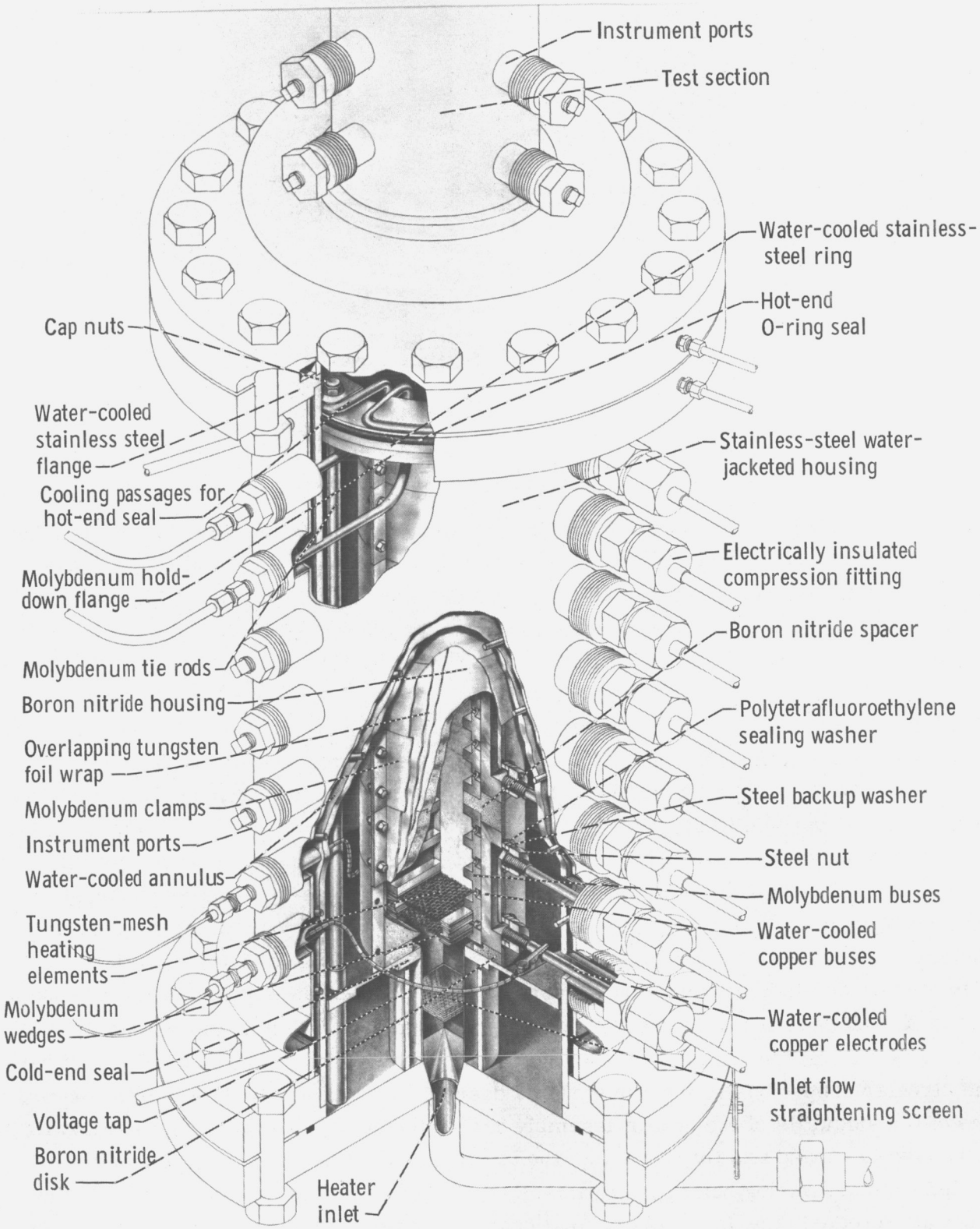

Figure 5. - Heater assembly with cutaway views of hot end and mesh bank assembly.

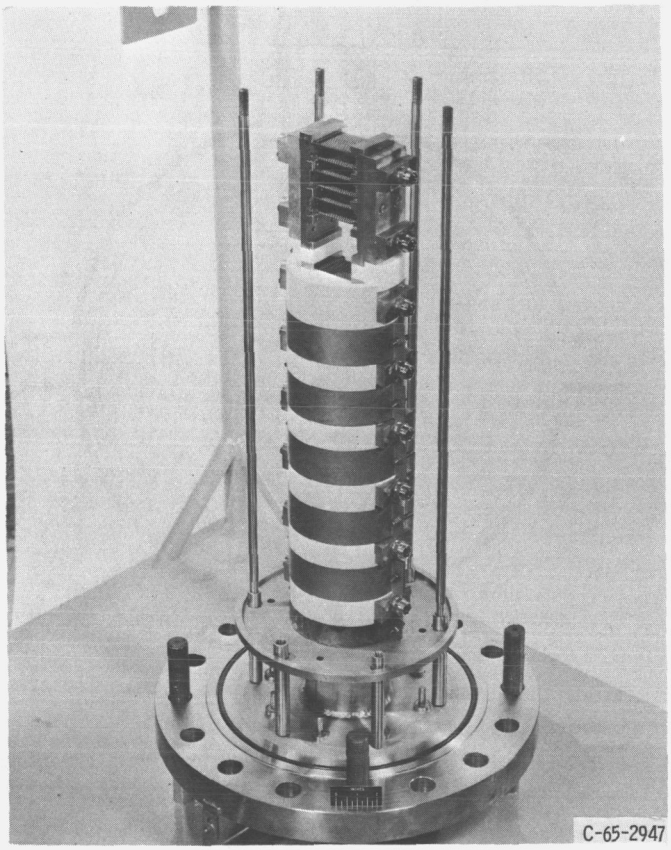

Figure 6. - Partly assembled heater.

heater design centers around minimization of this bypass and is the end result of several design modifications. To prevent the gas from escaping through axial gaps resulting from these expansion differences, the entire heater was wrapped in two overlapping 0.003-inch-thick (0.0076-cm-thick) sheets of tungsten foil. Figure 7 is a sketch of the heater cross section and wrap used to minimize axial bypass of the gas. These foil sheets extend along the entire length of the heater and completely surround the cylinder formed by the boron nitride housing and copper buses. To prevent the water-cooled copper buses from shorting against the foil, a thin sheet of an asbestos type of electrical insulating material was placed behind each bus. Molybdenum bands 0.036 inch (0.091 cm) thick and approximately $3\frac{1}{2}$ inches (8.89 cm) wide were clamped around the tungsten foil. The bands extend the entire length of the heater, as illustrated in figure 5 (p. 6). The local clamping enabled the foil to conform closely to the contour of the heater and minimize leakage. Provisions for sealing the heater where the 5/8-inch-diameter (1.59-cm-diam) copper tubes penetrate the tungsten sheet and clamps were also made. This seal was composed of a steel backup washer, a nut, and a polytetrafluoroethylene washer, one side of which was contoured to the shape of the heater housing. The nut screws onto

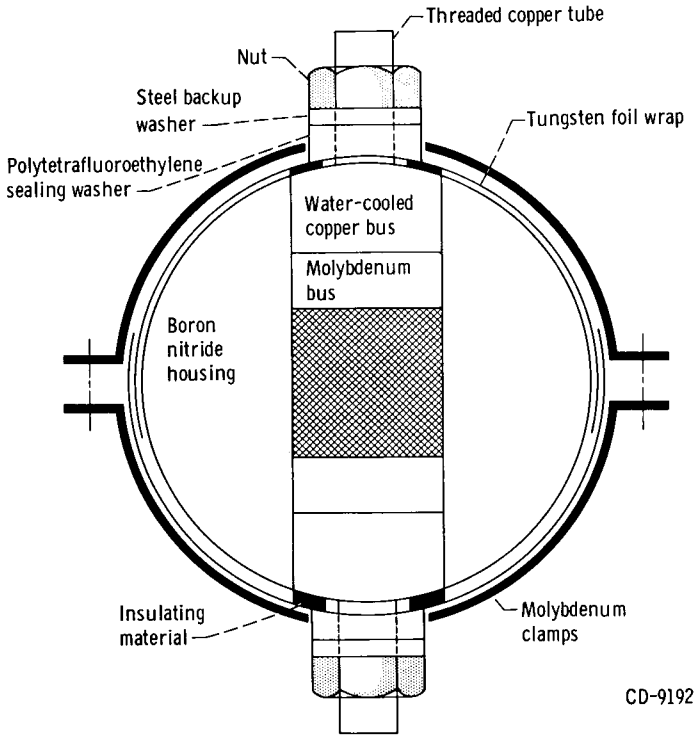

Figure 7. - Heater cross section showing tungsten foilwrap, molybdenum clamps, and electrode seals.

the threaded copper tube of the water-cooled copper bus and seals the polytetrafluoroethylene washer against the tungsten foil (fig. 7).

Cold and hot end seals are provided to assure that bypass of the gas is minimized. A rubber O-ring seal between the boron nitride disk and the stainless-steel plate provides the cold end seal. A rubber O-ring seal between a water-cooled stainless-steel ring and the pressure-vessel housing provides the hot end seal and is shown in the upper cutaway view of figure 5. This stainless-steel ring also seals against the molybdenum holddown flange. Cap nuts screwed onto six tie rods, four of which are shown in figure 6, tighten these plates down against the cylindrical heater assembly. Figure 8 shows the hot and cold end seals and the tungsten foil wrap used to seal against bypass. The molybdenum tie rods and clamps shown compress the heater assembly to minimize both axial and radial bypass. During operation the heater assembly can expand to some degree in the axial direction, and an equilibrium between the forces on the tie rods and heater will be reached.

The electrodes extending through the heater housing are 3/8-inch (0.952-cm) copper tubing with 1/16-inch (0.159-cm) walls. They are soldered to the inside of the 5/8-inch-diameter (1.59-cm-diam) threaded copper tubes shown in figure 3 (p. 4). The 3/8-inch (0.952-cm) electrodes are electrically insulated and pressure sealed where they penetrate the heater housing by a compression fitting.

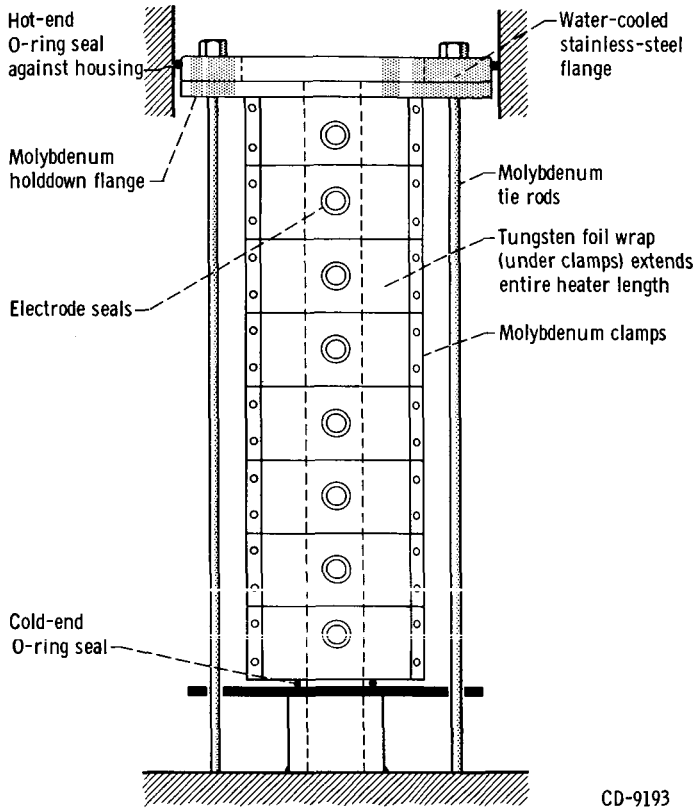

Figure 8. - Schematic diagram of heater assembly showing method of sealing against gas bypass.

Test Section

The test section was used to house experiments relating to the evaluation of fuel element configurations for the tungsten water-moderated reactor program. The water-jacketed test-section housing, which is located above the gas heater as shown in figure 1 (p. 2), has a 6-inch (15.2-cm) inside diameter and is 22 inches (55.9 cm) long. Figure 5 (p. 6) shows 4 of the 12 instrumentation ports located on the housing. The test-section housing was lined with cylindrically shaped zirconia fire bricks for insulation during the testing of the heater.

Flow Systems

As may be seen in figure 2 (p. 3), nitrogen is supplied to the flow system from a tube trailer at a maximum pressure of 2400 psi (1650 N/sq cm). From the trailer, the gas then flows through a remotely operated control valve, a choked flow nozzle, and an

on-off valve that supplies gas directly to the heater. The gas flow is metered by means of the choked flow nozzle that assures a constant mass flow through the test section as long as a choked condition is maintained in the nozzle for a constant upstream density. Three interchangeable nozzles are available to cover a range of nitrogen flow rates from 0.02 to 1 pound per second (0.0091 to 0.454 kg/sec). From the heater, the hot gas flows through a water-cooled test section and finally into a gas-to-water tube and shell heat exchanger, where it is cooled below 1500° R (833° K) before being exhausted into the atmosphere. A remotely operated back-pressure valve is located downstream of the heat exchanger. Its purpose is twofold, pressurizing the test section during operation and checking the pressure prior to operation.

There are two water flow systems associated with this facility, a cooling-tower water system and a city water system. The cooling-tower water system is used to cool the water-jacketed housings, flanges, and heat exchanger. In the heat exchanger the water flow is "two pass;" that is, it first flows counter to the gas through an annulus surrounding the shell, flows into a plenum, and then returns through the tubes. The single-pass gas flows through the heat exchanger between the water-cooled tubes and the water-jacketed shell.

The city water supply system, which contains less impurities than the cooling-tower water system, was used to cool the buses supplying electric power to the heaters. A flow schematic diagram typical for the water-cooled electric busing between a power supply output terminal block and a water-cooled copper bus of a heater bank is shown in detail in figure 2 (p. 3). Part of this busing is also shown in figure 1 (p. 2) and has the appearance of manometer boards. Each of these boards is composed of four 1/2-inch-thick (1.27-cm-thick) copper plates to minimize internal power generation within the tubing. As shown in figure 2, the water flows from the power supply output terminal block through two of these 1/2-inch-diameter (1.27-cm-diam) tubes into one electrode to the water-cooled copper bus of a heater bank and then returns to the same terminal block by flowing through the remaining two tubes. Grounding of the power supplies is prevented by the use of rubber insulating hoses between the city water supply and drain lines and the power supply output terminal blocks. The current flow is parallel in all four 1/2-inch-diameter (1.27-cm-diam) tubes.

A pump capable of a 125-psi (86-N/sq cm) outlet pressure is used to supply water at a flow rate of 8.5 gallons per minute (0.0322 cu m/min) through each heater electrode. Each of the parallel water flow loops supplying the electrodes and heater buses had hand valves for adjusting water flow rates through flowmeters located on the return side of the heater buses. Water-flow switches on the return side of busing shut down the power supplies in the event of an electrode failure.

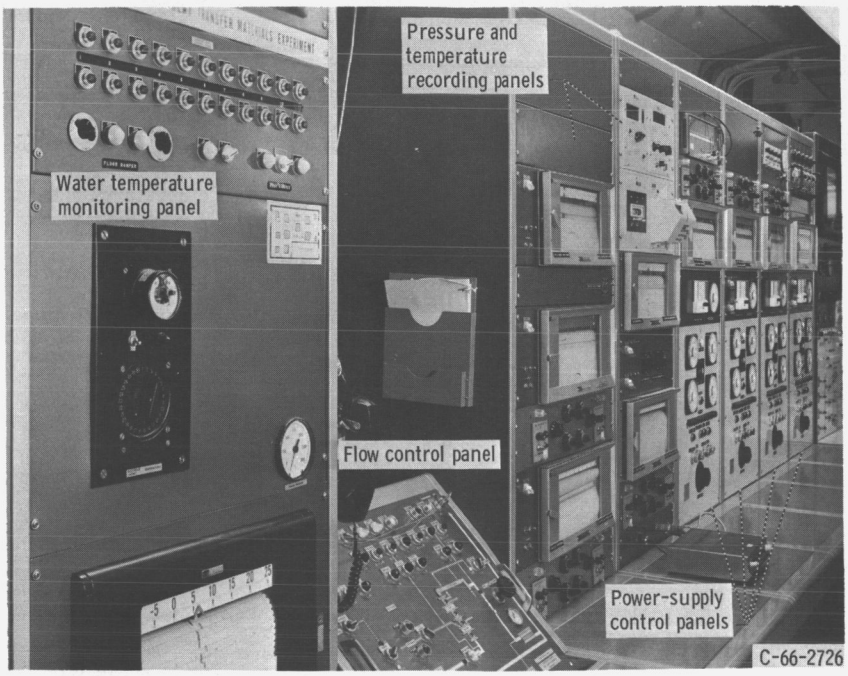

Figure 9. - Hot-gas-facility control panel.

Instrumentation

Figure 9 shows the control panel of the hot-gas facility. The panels shown from left to right are as follows: water temperature monitoring panel, flow control panel, pressure and temperature recording equipment panels, and four separate power supply control panels.

The instrumentation used is shown on the flow schematic diagram in figure 2 (p. 3). The current flowing through each stage of the heater was measured by a calibrated shunt having a 1-millivolt drop per 400 amperes. The voltage drop across a mesh bank was measured between the water-cooled copper buses of the heater and was read out on a digital voltmeter. Because of the heater design, it was difficult to measure voltages directly across the mesh. As a result, the mesh bank voltages include voltage drops due to contact resistances between the buses and mesh; however, prior tests have shown that these voltage drops are small. The total voltage is measured at the bus terminals of the power supplies.

The heater outlet gas temperature is calculated from a heat balance on the heat exchanger. The heat exchanger water-flow rate is measured with a calibrated orifice and its temperature rise with a differential iron-constantan thermocouple. Thermocouples were not used to measure heater outlet gas temperature because of (1) difficulties in obtaining a mixed average outlet gas temperature at these high flow rates and temperatures

and (2) difficulties in shielding the thermocouples from the hot mesh heating elements. Water temperatures entering and leaving water-jacketed housings and electrodes were individually measured by type K thermocouples (ref. 2).

The heater and test-section water jackets and electrode flow rates were individually measured by rotameters. A choked-flow nozzle was used to measure gas-flow rates. The gas-flow rate was set by adjusting the nozzle-inlet pressure for a given temperature. Constant gas flow was maintained provided that the exit pressure was not raised too high to unchoke the nozzle. The heater-inlet, heater-outlet, and nozzle-inlet static pressures were measured by temperature-compensated strain-gage bridge pressure transducers. All pressures, temperatures, and currents were continuously recorded on null balance potentiometer-type recorders.

Power Supplies

One of the four individually controlled silicon diode rectifiers is used to heat each bank of mesh. The specifications for each of these power supplies are as follows:

Power input	2400 V; three phase; 230 A ac
Rated power, kW, for -	
Continuous operation	540 (36 V at 15 000 A dc)
2-Hr operation	675 (36 V at 18 750 A dc)
Power output, kW	10 to 675
Output voltage, V	Adjustable from 3.6 to 36
Voltage control	Automatic within ±1 percent for preceding voltage range; achieved by magnetic amplifier control circuit
ac ripple	Maximum of 3 percent superimposed upon dc output at rated power

METHOD OF CALCULATION

Mesh Geometrical Parameters

The mesh heating elements are made of interwound helical tungsten coils. They can be completely specified by five parameters: wire diameter d, mandrel diameter D, number of parallel coils N, length of mesh b, and helical coil S, which is given by the equation

$$S = \frac{b}{p}\sqrt{\pi^2(D + d)^2 + p^2} \tag{1}$$

The total heat-transfer surface area for N number of coils is

$$A_s = \pi\, dSN \tag{2}$$

The equivalent diameter for porous media is normally defined as

$$D_e = \frac{4(\text{Void volume})}{A_s} = \frac{4LA_{f\ell}}{A_s} \tag{3}$$

where the average flow area is given as

$$A_{f\ell} = \epsilon bw$$

The porosity ϵ is defined as the average porosity for the entire mesh volume by

$$\epsilon = \frac{\text{Volume of mesh - Volume of tungsten in mesh}}{\text{Volume of mesh}} \tag{4}$$

The average surface temperature of the mesh was determined from the relation between temperature and resistivity of tungsten as given in reference 3. The resistivity ζ was calculated by

$$\zeta = \frac{V}{I}\,\frac{A}{S} \tag{5}$$

where A is the current flow cross-sectional area of the wire mesh for N' number of mesh and equals

$$A = \frac{N'N\pi d^2}{4}$$

The mesh geometrical parameters for each heater stage are given in table I.

TABLE I. - GEOMETRIC PARAMETERS FOR EACH MESH BANK

[Mandrel diam d, 0.080 in. (0.203 cm); mesh size b by w, 2.125 by 2 in. (5.40 by 5.08 cm); number of parallel coils per mesh N, 36.]

Parameter	Bank number			
	1	2	3	4
Wire diameter, d:				
in.	0.030	0.030	0.035	0.035
cm	0.0762	0.0762	0.0889	0.0889
Equivalent diameter, D_e:				
in.	0.071	0.071	0.065	0.065
cm	0.180	0.180	0.165	0.165
Coil pitch, p:				
in./turn	0.111	0.111	0.125	0.125
cm/turn	0.282	0.282	0.318	0.318
Porosity, volume of void/ total volume of mesh	0.703	0.703	0.65	0.65
Number of meshes per bank, N'	6	8	8	8

Mesh Heating Element Design

The mesh used in the design of the heater was determined by an iterative process using the following equations:

$$Q = WC_p(T_{out} - T_{in}) \tag{6}$$

$$Q = hA_s\left(T_w - \frac{T_{out} + T_{in}}{2}\right) \tag{7}$$

$$Q = K\frac{V^2}{R} \tag{8}$$

where the heat-transfer coefficient h is calculated from the correlation as reported in reference 1.

$$\frac{hD_e}{k_s} = 0.462\left(\frac{WD_e}{A_{f\ell}\mu_s}\right)^{0.53}\left(\frac{C_p\mu}{k}\right)_s^{0.40} \tag{9}$$

The gas properties used were taken from reference 4.

The flow rate W and the inlet temperature to the bank T_{in} are known. With the mesh connected electrically in parallel, the voltage V can be taken as that available to the mesh from the power supply. Initially the mesh parameters A_s, $A_{f\ell}$, and D_e have to be specified. Since the heat-transfer coefficient h and the resistance R are both functions of the surface temperature, when the mesh parameters are specified, the only remaining unknowns are Q, T_{out}, and T_w.

The heat-transfer characteristics of the first mesh of the bank, where T_{in} is known, can then be calculated by an iterative process using equations (6) to (8). The heat-transfer characteristics of the second mesh element of the bank can be calculated by using the outlet gas temperature from the first mesh as the inlet gas temperature to the second. To determine the number of mesh in the bank, this iterative process is repeated with an additional identical mesh heating element added each time until either of two limitations occur: (1) the surface temperature of the last mesh calculated exceeds the desired limiting value, or (2) the total current through all the meshes of one bank exceeds that available from the power supply.

The initial choice of mesh parameters may not provide a satisfactory solution. However, by varying the mesh parameters and repeating this procedure, an optimization of the resistance match between the mesh bank and power supply can be achieved with a mesh surface temperature approaching the desired limiting value.

System Heat Balance

A heat balance on the entire system was obtained by a comparison between the electrical output of the power supplies and the heat picked up in all the water flow systems and the residual heat in the exhaust gas.

$$K(P_1 + P_2 + P_3 + P_4) = \underbrace{W_1 C_{p,w} \Delta T_1}_{\text{Heat exchanger}} + \underbrace{W_2 C_{p,w} \Delta T_2}_{\text{Electrodes}} + \underbrace{W_3 C_{p,w} \Delta T_3}_{\text{Water jackets}} + \underbrace{W C_{p,e} (T_3 - T_1)}_{\text{Residual heat remaining in heat exchanger exhaust gas}} \tag{10}$$

A comparison of the right and the left sides of equation (10) indicates how good the overall heat balance is.

The outlet gas temperature from the heater can be calculated by equating the heat added to the gas by the heater to the heat removed from the gas by the water in the heat exchanger plus that residual heat remaining in the exhaust gas.

$$WC_{p,h}(T_2 - T_1) = W_1 C_{p,w} \Delta T_1 + WC_{p,e}(T_3 - T_1) \tag{11}$$

$$T_2 = \frac{W_1 C_{p,w} \Delta T_1 + WC_{p,e}(T_3 - T_1)}{WC_{p,h}} + T_1 \tag{12}$$

Since there was no measurable rise in the water temperature flowing through the test-section water jacket, because of the good thermal insulating properties of the zirconia fire bricks, the temperature of the gas entering the heat exchanger and leaving the heater are the same.

DISCUSSION OF HEATER OPERATION

The final heater design described under the section, DESCRIPTION OF GAS-HEATER FACILITY, was obtained by several modifications of the initial design. The most difficult problem area was that of gas bypass around the heater mesh. The original heater design, which had only a cold end seal, sealed when pressure checked at room temperature. However, differences in the relative expansion rates of the materials and axial temperature gradients during operation caused considerable bypass. This condition was evident from the very low power requirements of the three upper banks of the heater in comparison with the first bank, which was adjacent to the cold end seal. Figure 10 (taken from ref. 1) illustrates the effect of bypass flow area quite well. For example, figure 10 shows that for a bypass flow area of 25 percent, the heat transferred to the gas is reduced by 45 percent at a value of $(T_s/T_1) - 1$ of 6. The success of the modified heater design can be attributed to the ability of minimizing this bypass flow area. This was accomplished in two ways: (1) using both a hot and a cold end seal and (2) surrounding the heater completely with a tungsten wrap.

Another problem area was the water-cooled copper electrodes which supply the electric power to the water-cooled heater buses from the busing located outside the heater housing. Initially, large-diameter heavy wall electrodes were used to minimize the power generation within them, but a combination of induced thermal stresses and low water velocities, resulting in a low heat-transfer coefficient, caused rupture or electrode burnout on numerous occasions. In the final design two 3/8-inch-outside-diameter (0.952-cm-o.d.) 1/16-inch (0.159-cm) wall copper electrodes were used to carry the

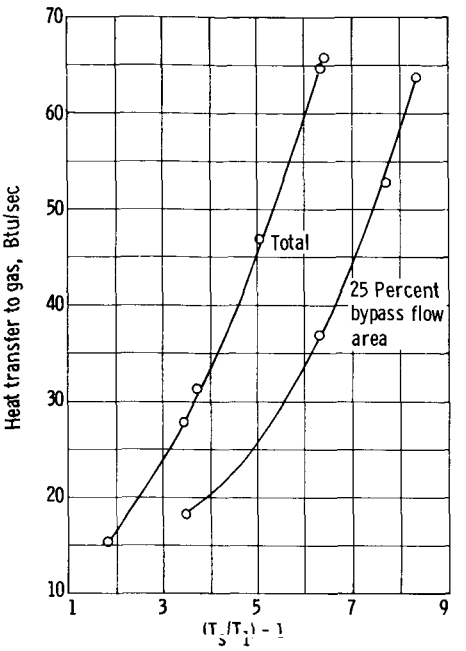

Figure 10. - Comparison of heat transfer to gas with and without bypass from experimental data. Gas flow rate, 0.0199 pound per second (0.00904 kg/sec); inlet gas temperature, 520° R (289° K); gas, hydrogen. (Figure taken from ref. 1.)

total power supply current of 18 750 amperes. With an electrode water flow rate of 8.5 gallons per minute (0.0322 cu m/min), the electrode outlet water temperature never exceeded 630° R (350° K). These small electrodes were desirable for two reasons: (1) since the electrodes are perpendicular to the axis of the heater and are fixed between the buses and the housing, they are more flexible to accommodate thermal expansion of the heater assembly than larger electrodes; and (2) the water velocities are higher and result in less chance of boiling burnout occurring.

An important advantage of this type of heater is that the mesh of a bank of this design can operate at an average surface temperature close to the maximum operating temperature. The reason becomes apparent when it is realized that the mesh of a heater bank is electrically connected in parallel and in series with the gas flow; that is, the gas temperature progressively increases in the flow direction through the mesh, and the voltage drop across each mesh is the same. Since the electrical resistance of tungsten increases with temperature, and the last mesh runs hotter than the first, because of the increasing gas temperature, the current and power generated in the mesh progressively decreases downstream of the first mesh. The result is a self-limiting effect that tends to even out the mesh temperatures within any bank and enables the mesh to operate at a higher average surface temperature than otherwise possible. This higher average surface temperature allows more heat to be transferred, if the heat-transfer coefficient

is assumed to remain the same, and results in a higher outlet gas temperature for the same peak surface temperature. However, if a higher outlet gas temperature is not desired, the peak surface temperature of the mesh can be considerably reduced with an increase in heater life.

Another important advantage of mesh elements is that thermal expansion does not create a problem. Although the ends are fixed between the two molybdenum buses, the mesh is free to expand by bowing. As mentioned in reference 1, bowing had no apparent effect on the heat-transfer characteristics of the mesh. In comparison, providing for expansion in a rigid heating element may be a problem.

The number of mesh and the wire size were increased for each successive bank of meshes to utilize the maximum capabilities of the power supplies and to compensate for the change in electrical resistivity of the mesh with increasing gas temperature. Table I (p. 14) gives the mesh arrangements used in the heater and the geometric parameters associated with each.

Table II summarizes the test data of five runs of this heater with all four banks operating. Two nitrogen flow rates of 0.45 and 0.69 pound per second (0.204 and 0.314 kg/sec) were used. The highest outlet gas temperature of 4530° R (2520° K) was obtained for run 3 with a flow rate of 0.45 pound per second (0.204 kg/sec). The average surface temperature of the banks varied from 3080° R (1710° K) for the first bank to 4430° R (2460° K) for the last bank. A 1-hour run under these conditions has been achieved without failure of the heater.

A maximum total power output of 1586 kilowatts from the power supplies was obtained for run 5 at a flow rate of 0.69 pound per second (0.314 kg/sec) and an outlet gas temperature of 4200° R (2330° K). The electric power input varied from 496 kilowatts on the first bank down to 265 kilowatts on the fourth bank. The power input to the gas was 760 kilowatts. The overall heat balance was obtained by comparing the measured heat picked up by the cooling water and the residual heat remaining in the gas to the electric power input, as in equation (10). The ratio of these varied from 0.940 to 1 and indicated that a good overall heat balance was obtained.

The mesh heater proved to be very successful when nitrogen was used as the coolant gas. This heater could also be used with other gases that are nonoxidizing. If hydrogen is used in this heater, no difficulties are anticipated, since hydrogen was used in obtaining the single mesh heat-transfer correlation reported in reference 1. However, during initial testing of the heater elements, when helium was used as the heat-transfer fluid, considerable mesh hot spotting and subsequent burnout at low average mesh surface temperatures occurred. In an effort to determine the cause of heater failure when helium was used, argon was substituted as the coolant. (Helium and argon are both monatomic.) No hot spotting or burnout of the mesh occurred. The puzzling results obtained with helium provided the motivation for investigating noninterwound meshes

TABLE II. - HIGH-TEMPERATURE TUNGSTEN-MESH GAS-HEATER

[Total electrode water flow rate W_2, 9.45 lb/sec (4.29 kg/sec).]

Property	Run				
	1	2	3	4	5
Heater-inlet gas temperature, T_1:					
^oR	545	545	535	535	530
^oK	303	303	297	297	294
Heater-outlet gas temperature, T_2:					
^oR	3070	3890	4530	3800	4200
^oK	1710	2160	2520	2110	2330
Heat-exchanger-outlet gas temperature, T_3:					
^oR	742	814	870	945	1015
^oK	412	452	483	525	564
Heater-inlet pressure, p_1:					
psia	120	125	130	187	192
N/sq cm	83	86	90	129	132
Heater-outlet pressure, p_2:					
psia	45	45	48	78	79
N/sq cm	31	31	33	54	54
Nitrogen flow rate, W:					
lb/sec	0.462	0.458	0.450	0.703	0.69
kg/sec	0.210	0.208	0.204	0.319	0.314
Average rise in electrode water temperature, ΔT_2:					
^oR	55	57	57	72	68
^oK	30.6	31.7	31.7	40	37.8
Total water jacket flow rate, W_3:					
lb/sec	5.14	5.14	5.14	5.56	5.56
kg/sec	2.33	2.33	2.33	2.52	2.52
Average rise in water jacket temperature, ΔT_3:					
^oR	7.0	7.0	7.5	7.0	8.5
^oK	3.9	3.9	4.2	3.9	4.7
Heat-exchanger water flow rate, W_1:					
lb/sec	10.43	10.43	10.43	10.56	10.7
kg/sec	4.73	4.73	4.73	4.79	4.85
Rise in heat-exchanger water temperature, ΔT_1:					
^oR	29.0	39.4	47.0	55.8	61.2
^oK	16.1	21.9	26.1	31.0	34.0
Current, I_1, A	14 600	14 500	15 100	16 800	16 800
Current, I_2, A	13 700	14 300	13 800	16 400	16 300
Current, I_3, A	14 500	15 500	15 800	17 400	17 800
Current, I_4, A	14 700	14 500	13 400	16 600	14 400
Mesh voltage drop, V_1, V	9.0	10.4	13.5	14.3	18.0
Mesh voltage drop, V_2, V	7.6	9.8	11.6	13.7	15.2
Mesh voltage drop, V_3, V	5.8	8.5	10.3	10.1	11.7
Mesh voltage drop, V_4, V	6.6	9.5	9.5	10.7	9.8
Power supply input, P_1, kW	271	280	355	430	496
Power supply input, P_2, kW	224	270	272	385	415
Power supply input, P_3, kW	214	280	310	365	410
Power supply input, P_4, kW	228	246	228	332	265
Total power input, kW	937	1076	1165	1512	1586
Average mesh bank surface temperature, $T_{s,1}$:					
^oR	2250	2560	3080	2950	3580
^oK	1250	1420	1710	1640	1990
Average mesh bank surface temperature, $T_{s,2}$:					
^oR	2610	3125	3700	3680	4030
^oK	1450	1730	2060	2040	2240
Average mesh bank surface temperature, $T_{s,3}$:					
^oR	2750	3570	4120	3740	4150
^oK	1530	1980	2290	2080	2310
Average mesh bank surface temperature, $T_{s,4}$:					
^oR	3020	4140	4430	4090	4270
^oK	1680	2300	2460	2270	2370

reported in reference 5. The cause of hot spotting, when helium was used, as reported in this reference was attributed to a combination of the following factors: (1) nonuniformities in the interwound geometry which resulted in flow maldistribution within the matrix and (2) the high heat fluxes associated with helium because of its high heat capacity. While even higher heat fluxes result with the use of hydrogen as the heat-transfer fluid, the increase in heat transfer resulting from the dissociation of hydrogen above 3500° R (1945° K) compensate for this and permit the mesh to operate at near-uniform surface temperatures above 4000° R (2220° K). Reference 5 also shows that by using noninterwound mesh and helium as a coolant, average mesh surface temperatures as high as 4000° R (2220° K) can be achieved. Since the use of helium in this heater is not anticipated, noninterwound mesh has not been considered. However, based on the results of reference 5, helium gas temperatures as high as those obtained with nitrogen could probably be attained with noninterwound mesh.

At the time of this report, approximately 15 hours of heater operation has been logged with no apparent change in mesh wire diameter due to oxidation or metal vaporization. The data reported in table II (p. 19) are not the maximum test conditions possible. So far, no attempt has been made to find the maximum outlet gas temperature attainable or the maximum average surface temperature for a mesh life of at least 1 hour. However, during one of the initial tests on a bank consisting of six meshes, an average surface temperature above 5200° R (2890° K) was attained before failure. Based on past experience, it is felt that the last bank of meshes in the heater could operate at an average temperature of 5000° R (2780° K) for 1 hour.

CONCLUDING REMARKS

A high-temperature electrical gas heater was designed and is operational. The heater consists of four banks of electrically heated interwound tungsten mesh heating elements, with each bank containing six to eight mesh elements. The heater has heated 0.45 pound per second (0.204 kg/sec) of nitrogen to 4530° R (2520° K) and has operated continuously under this condition for 1 hour. A nitrogen flow rate of 0.69 pound per second (0.314 kg/sec) has been heated to 4200° R (2330° K) with this heater. A total of 15 hours of operation have been logged at the time of this report without failure. Since no failure has occurred, the maximum capabilities of the heater are undefined.

The tungsten mesh elements used in this heater design offer several advantages, which are as follows:

1. The mesh elements can operate at nearly constant surface temperature from heater inlet to outlet. Much higher outlet gas temperatures are thereby obtained for any given peak surface temperature.

2. No serious expansion problem exists. The mesh, though clamped at both ends, is free to expand by bowing. No measurable change in heat-transfer characteristics of the mesh occurs as a result of bowing.

3. The mesh is commercially available and is easily fabricated. In addition, it can be made to match various resistance requirements; thus, a considerable degree of design flexibility is available.

Bypassing of the gas around the mesh is extremely critical and has to be almost entirely eliminated for the heater to operate properly. This was achieved by hot and cold end seals and a tungsten foil wrap completely surrounding the heater assembly.

The heater can be used with nitrogen, helium, hydrogen, or argon as the heat-transfer fluid. However, it would be desirable to substitute noninterwound mesh if helium were to be used.

Lewis Research Center,
National Aeronautics and Space Administration,
Cleveland, Ohio, July 25, 1967,
120-27-04-56-22.

APPENDIX - SYMBOLS

A	current flow cross-sectional area of mesh bank, sq in.; sq cm
$A_{f\ell}$	mesh free-flow area, sq in.; sq cm
A_s	mesh surface area, sq in.; sq cm
b	length of mesh, in.; cm
C_p	specific heat of gas at constant pressure, Btu/(lb)(^oR); J/(kg)(^oK)
$C_{p,e}$	average specific heat of residual gas at constant pressure, Btu/(lb)(^oR); J/(kg)(^oK)
$C_{p,h}$	average specific heat of gas in heater at constant pressure, Btu/(lb)(^oR); J/(kg)(^oK)
$C_{p,w}$	specific heat of water at constant pressure, Btu/(lb)(^oR); J/(kg)(^oK)
D	mandrel diameter, in.; cm
D_e	equivalent diameter, in.; cm
d	wire diameter, in.; cm
h	heat-transfer coefficient, Btu/(sec)(sq in.)(^oR); J/(sec)(sq cm)(^oK)
I	current, A
K	conversion constant for electric to thermal heat
k	thermal conductivity of gas, Btu/(in.)(sec)(^oR); J/(cm)(sec)(^oK)
N	number of parallel coils per mesh
N'	number of meshes per bank
P	total electric power input per power supply, kW
p	coil pitch, in./turn; cm/turn
p_1	heater-inlet static pressure, psia; N/sq cm abs
p_2	heater-outlet static pressure, psia; N/sq cm abs
Q	heat transferred from a mesh heating element to gas, Btu/sec; J/sec
R	resistance of a mesh heating element, ohms
S	total wire length of helical coil, in.; cm
T_{in}	inlet gas temperature to mesh, ^oR; ^oK
T_{out}	outlet gas temperature from mesh, ^oR; ^oK

T_s average mesh surface temperature per bank, ^{o}R; ^{o}K

T_w average surface temperature of a mesh, ^{o}R; ^{o}K

T_1 heater-inlet temperature, ^{o}R; ^{o}K

T_2 heater-outlet temperature (heat-exchanger-inlet temperature), ^{o}R; ^{o}K

T_3 heat-exchanger-outlet gas temperature, ^{o}R; ^{o}K

ΔT_1 heat-exchanger water temperature rise, ^{o}R; ^{o}K

ΔT_2 electrode water temperature rise, ^{o}R; ^{o}K

ΔT_3 water-jacket water temperature rise, ^{o}R; ^{o}K

V mesh voltage drop, V

W gas flow rate, lb/sec; kg/sec

W_1 heat-exchanger water flow rate, lb/sec; kg/sec

W_2 total electrode water flow rate, lb/sec; kg/sec

W_3 total water-jacket water flow rate, lb/sec; kg/sec

w mesh width, in.; cm

ϵ mesh porosity

ζ resistivity of tungsten, ohm-in.; ohm-cm

μ absolute viscosity of gas, lb/(sec)(in.); N/(sec)(cm)

Subscripts:

s gas properties evaluated at average surface temperature

1 mesh bank 1 (except where otherwise noted)

2 mesh bank 2 (except where otherwise noted)

3 mesh bank 3 (except where otherwise noted)

4 mesh bank 4 (except where otherwise noted)

REFERENCES

1. Siegel, Byron L.; Maag, William L.; Slaby, Jack G.; and Mattson, William F.: Heat-Transfer and Pressure Drop Correlations for Hydrogen and Nitrogen Flowing Through Tungsten Wire Mesh at Temperatures to 5200° R. NASA TN D-2924, 1965.
2. Anon.: Thermocouples and Thermocouple Extension Wires. Rev. Composite of RPI. 9-RPI. 7, Instr. Soc. Am., July 1959.
3. Anon.: Temperature: Its Measurement and Control in Science and Industry. Reinhold Publishing Corp., 1941, p. 1318.
4. Hilsenrath, Joseph, et al.: Tables of Thermal Properties of Gases. Circ. 564, National Bureau of Standards, Nov. 1, 1955.
5. Maag, William L.; and Mattson, William F.: Forced-Convection Heat-Transfer Correlations for Gases Flowing Through Wire Matrices at Surface Temperatures to 5500° R. NASA TN D-3956, 1967.

NASA-Langley, 1967 —— 22 E-3874